Published in final edited form as:
J Muscle Res Cell Motil. 2010 September ; 31(3): 163–170. doi:10.1007/s10974-010-9220-y.

Nonmuscle myosin IIA with a GFP fused to the N-terminus of the regulatory light chain is regulated normally

Andras Kengyel,
Laboratory of Molecular Physiology, National Heart, Lung and Blood Institute, National Institutes of Health, Building 50, Room 3523, Bethesda, MD 20892, USA. Department of Biophysics, Faculty of Medicine, University of Pécs, Pécs, Hungary

Wendy A. Wolf,
Center for Genetic Medicine, Feinberg School of Medicine, Northwestern University, Chicago, IL 60611, USA

Rex L. Chisholm, and
Center for Genetic Medicine, Feinberg School of Medicine, Northwestern University, Chicago, IL 60611, USA

James R. Sellers
Laboratory of Molecular Physiology, National Heart, Lung and Blood Institute, National Institutes of Health, Building 50, Room 3523, Bethesda, MD 20892, USA

James R. Sellers: Sellersj@nhlbi.nih.gov

Abstract

Nonmuscle myosin II plays a crucial role in a variety of cellular processes (e.g., polarity formation, cell motility, and cytokinesis). It is composed of two heavy chains, two regulatory light chains and two essential light chains. The ATPase activity of the myosin II motor domain is regulated through phosphorylation of the regulatory light chain (RLC) by myosin light chain kinase. To study myosin function and localization in cellular processes, GFP-fused RLCs are widely used; however, the exact kinetic properties of myosins with bound GFP-RLC are poorly described. More importantly, it has not been shown that a regulatory light chain fused at its N-terminus with GFP can maintain the normal phosphorylation-dependent regulation of nonmuscle myosin or serve as a substrate for myosin light chain kinase. We coexpressed N-terminal GFP-RLC with a heavy meromyosin (HMM)-like fragment of nonmuscle myosin IIA and essential light chain to characterize the phosphorylation dynamics and in vitro kinetic properties of the resulting HMM. Myosin light chain kinase phosphorylates the GFP-RLC bound to HMM IIA with the same V_{max} as it does the wild type RLC bound to HMM IIA, but the K_m is about two fold higher for the GFP fusion protein, meaning that it is a somewhat poorer substrate. The steady-state actin-activated MgATPase activity of the GFP-RLC HMM is very low in the absence of phosphorylation demonstrating that the GFP moiety does not prevent formation of the off state. The actin-activated MgATPase activity of phosphorylated GFP-RLC-HMM and is about half that of wild type phosphorylated HMM. The ability of phosphorylated GFP-RLC-HMM to move actin filaments in the actin gliding assay is also slightly compromised. These data indicate that despite some kinetic differences the N-terminal GFP fusion to the regulatory light chain is a reasonable model system for studying myosin function in vivo.

Correspondence to: James R. Sellers, Sellersj@nhlbi.nih.gov.

Keywords

GFP; Nonmuscle myosin; Regulatory light chain; Enzymatic activity; In vitro motility

Introduction

Nonmuscle myosin IIA is an actin-dependent molecular motor protein that plays important roles in a variety of cellular processes, including cytokinesis, chemotaxis, cell migration, and stress fiber formation, or polarity formation (Sellers, 2000; Vicente-Manzanares et al. 2009). Like other conventional myosins, it consists of two identical heavy chains, each composed of three domains. There is an N-terminal motor domain responsible for actin binding and the enzymatic activity, a neck region, which binds the essential light chain (ELC) and the regulatory light chain (RLC) and a C-terminal tail domain, consisting predominantly of coiled-coil forming sequences which dimerize the two heavy chains. The soluble form of myosin, which is well suited for kinetic studies, is the dimeric heavy meromyosin (HMM), which lacks the distal two-thirds of the tail domain. This fragment was historically prepared by limited proteolysis of myosin, but HMM-like fragments can be easily engineered for expression in the Sf9/baculovirus system (Sellers et al. 1988; Wang et al. 2000).

The MgATPase activity of the motor domain is primarily switched on by the phosphorylation of Ser19 of the RLC by the calcium/calmodulin dependent myosin light chain kinase (MLCK) (Sellers, 1991). This phosphorylation results in a marked increase in actin-activated myosin MgATPase activity and promotes myosin IIA filament assembly (Sellers, 1991; Vicente-Manzanares et al. 2009). However, myosin IIA regulation in vivo is a complex equilibrium between phosphorylation and dephosphorylation by various kinases and phosphatases, such as MLCK, Rho-kinase, ZIP-kinase and myosin light chain phosphatase (MLCP) (Bresnick, 1999; Vicente-Manzanares et al. 2009).

To study the localization of myosins in vivo, cells are often transfected with constructs in which RLC is fused with GFP on its C-, or N-terminus. When transiently expressed in cells these fluorescently tagged fusion proteins bind to the myosin heavy chain in place of the endogenous RLC and report the localization of myosin (Bajaj et al. 2009; Komatsu et al. 2000; Peterson et al. 2004; Uchimura et al. 2002). It was shown that C-terminal GFP-tagged RLC could be incorporated into myosin and this myosin was activated significantly by phosphorylation (Komatsu et al. 2000). The question of whether the 20 kDa RLC, if fused at its N-terminus with a 28 kDa GFP, can also function properly and whether it displays normal regulation remains unanswered. In our present work we coexpressed HMM IIA and N-terminal GFP-RLC and ELC in the baculovirus/Sf9 system. The ability of the purified protein to serve as a substrate for MLCK and its interaction with actin was characterized. The data show some minor differences between the function of the HMM containing GFP-RLC compared to WT-HMM, but the ability of this chimeric light chain to regulate the activity of the myosin was still intact. Based on these in vitro kinetic studies, we believe that the in vivo behavior of nonmuscle myosin containing the N-terminal GFP-RLC chimera should be sufficiently similar to that of WT-non-muscle myosin to justify its use as a fluorescent reporter of myosin localization in cell biological studies.

Materials and methods

Protein expression and purification

The mouse nonmuscle RLC GFP fusion was produced by PCR amplification of a full length mouse nmRLC cDNA using a 5′ primer to add a BglII site and a 3′ primer to add a Pst I site.

The BglII-nmRLC-PstI fragment was cloned into the pEGFP-CI vector (Clontech) between the BamHI and PstI sites. This produces a fusion protein with the structure GFP-SGLRS-nmRLC, which was then cloned into baculovirus. The resulting construct was sequenced to assure that PCR amplification did not introduce any sequence changes into the nmRLC.

Recombinant human nonmuscle heavy meromyosin IIA (HMM IIA) with an N-terminal Flag tag was co-expressed with mouse nonmuscle regulatory light chain fused with a GFP on its N-terminus (GFP-RLC) and with bovine non-muscle essential light chain (ELC) in the baculovirus/Sf9 expression system (Kovacs et al. 2003). For control experiments HMM IIA was coexpressed with the baculovirus containing both the WT-RLC and the ELC. The infected Sf9 cells were harvested by sedimentation after 72 h of growth and stored at −80 °C. HMM IIA was purified as described by Wang et al. (2000). Briefly, the cell pellets were extracted and homogenized in a buffer containing 0.5 M NaCl, 10 mM MOPS (pH 7.3) 10 mM $MgCl_2$, 1 mM EGTA, 3 mM NaN_3, 2 mM ATP, 0.1 mM phenylmethylsulfonyl fluoride, 0.1 mM dithiothreitol, 5 μg/ml leupeptin, and proteinase inhibitor mixture (Invitrogen). The HMM IIA copurified with the light chains by the Flag-affinity chromatography using M2 Flag affinity gel (Sigma) and was concentrated on a Mono-Q Sepharose column using FPLC (Amersham).

The MLCK used in this study was provided by Mary Anne Conti (NHLBI) or Mitsuo Ikebe (University of Massachusetts).

Phosphorylation assay

HMM IIA with either WT-RLC or GFP-RLC at 0.9 μM was phosphorylated at various MLCK concentations at 25 °C in a reaction mixture containing 10 mM MOPS, pH 7.3, 50 mM KCl, 5 mM $MgCl_2$, 0.2 mM $CaCl_2$, 0.1 mM EGTA, 0.1 μM calmodulin, 1 mM DTT, and 0.2 mM ATP. After starting the reaction, 10 μg myosin samples were taken at different time points, precipitated immediately in cold acetone and sedimented at 16000 g for 5 min. The myosin pellets were dissolved in tris–glycine buffer (pH 8.6) containing 8 M urea, 0.54 M mercaptoethanol. The unphosphorylated and phosphorylated light chains could be separated by gel electrophoresis using 40% glycerol–10% polyacrylamide gel (Facemyer and Cremo, 1992). The phosphorylation state was analyzed with densitometry, using Licor Odyssey software, by calculating the ratio of the density of the phosphorylated light chain and the total density of the phosphorylated and unphosphorylated light chains at each time point.

Alternatively, HMM IIA with either WT-RLC or GFP-RLC was phosphorylated in the same conditions described above, but using 0.2 mM [γ-^{32}P]ATP (Nishikawa et al. 1984). The assay was initiated by addition of 0.9 μM myosin. Samples (20 μl) were taken at every time point and were applied to Whatman Grade3 (Ø 23 mm) filter paper discs, which were immediately immersed in 5% trichloroacetic acid containing 2% sodium pyrophosphate. The filter paper discs were washed in this solution 4 times for 10 min to remove any non-specifically bound isotopes and finally with 100% ethanol for 10 min. The incorporation of ^{32}P into the protein was determined by counting the samples in a Beckman LS6500 Scintillation Counter.

Phosphorylation kinetics were assayed in the same reaction buffer as described above, using various myosin concentrations and 0.1 nM MLCK. Samples for each myosin concentration were taken after 60, 120, 180, and 240 s and processed as described above for scintillation counting. The data were fit with a linear regression to determine the initial rate.

Steady-state ATPase activities were measured at various actin concentrations using an NADH-coupled assay at 25 °C in a low ionic strength buffer (Wang et al. 2003).

Experimental conditions were: 10 mM MOPS (pH 7.0), 2 mM $MgCl_2$, 0.2 mM $CaCl_2$, 0.1 mM EGTA, 1 μM cal-modulin, 2 mM ATP, 40 U/ml lactate-dehydrogenase, 200 U/ml pyruvate-kinase, 1 mM phosphoenolpyruvate, and 200 μM NADH. The basal activity of the myosins were measured in the absence of MLCK, then RLC phosphorylation was initiated by adding 28 nM myosin light chain kinase (MLCK). Data was collected with a Beckman Coulter spectrophotometer and analysed with the Origin statistical program. The Michaelis–Menten kinetic constants, V_{max} and K_m, where calculated by fitting the Michaelis–Menten equation to the data points. Before performing the steady-state ATPase assay, the myosin was cosedimented with phalloidin-stabilized actin and then the functionally active myosin heads were released from actin by the addition of ATP. There were less than 5% inactive, rigor-like molecules for both WT and GFP-RLC-HMM IIA (data not shown).

In vitro motility assay was performed as previously described (Sellers, 2001). Immediately prior to the start of motility assay 1–2 mg/ml HMM was mixed with 5 μM phalloidin-stablized actin and 1 mM MgATP and sedimented for 7 min at 470,000 Xg. The supernatant from this sedimentation was used as the source of HMM. This removes inactive myosin heads which bind to actin in an ATP-independent manner which would interfere with smooth motility of the actin filaments. Briefly, a flow chamber constructed on a microscope slide was filled with 0.1–0.2 mg/ml myosin and was incubated for 1 min to allow myosin to adhere to the nitrocellulose coated surface. The nitrocellulose surface was then blocked with 1 mg/ml BSA in motility buffer containing 50 mM KCl, 20 mM MOPS (pH 7.4), 0.1 mM EGTA, and 5 mM $MgCl_2$. After washing the chamber with motility buffer, 20 nM TRITC-phalloidin labeled F-actin in motility buffer was applied to the flow chamber. Finally the chamber was washed with the assay mix containing, 0.35% methylcellulose, 50 mM DTT and 1 mM ATP in motility buffer with the addition of 2.5 mg/ml glucose, 0.05 mg/ml glucose oxidase and 2 μg/ml catalase to retard photobleaching. Motility started only after phosphorylating the RLC using the assay mix containing 0.2 mM $CaCl_2$, 0.1 μM calmodulin and 28 nM MLCK. Images were taken with Zeiss Axioplan microscope and analyzed according to Homsher et al. (1992).

Results

Expression and purification of GFP–HMM IIA

We have previously characterized the enzymatic and motile properties of an HMM-like fragment of nonmuscle myosin IIA co-expressed with a regulatory (RLC) and essential (ELC) light chain in the baculovirus/Sf9 insect cell expression system (Kovacs et al. 2003). The heavy chain was tagged at the C-terminus with the Flag epitope to facilitate affinity chromatographic purification. We have now co-expressed this heavy chain construct with a GFP-fused regulatory light chain and an essential light chain. The GFP was fused to the N-terminus of the RLC. Approximately 5 mg of protein could be purified from 10^9 Sf9 cells. The protein was stable on ice, and no degradation was detectable for at least one week. The components of the GFP-RLC-HMM construct were confirmed by western blot using anti-Flag (Sigma), anti-GFP (Proteus Biosciences) and anti-ELC (AbCam) commercially available antibodies (Fig. 1a). Based on densitometry, GFP-RLC and ELC copurify with HMM IIA monomers in a stochiometric ratio, indicating that the GFP-RLC properly assembles with the HMM IIA heavy chain. However, a small amount (< 5%) of protein that co-migrates with the WT-RLC is also seen, which could be either a cleaved product of the GFP-RLC or the endogenous RLC picked up from the Sf9 cells. As control in every experiment, we used WT-HMM IIA, which was coexpressed, with RLC lacking the GFP tag and ELC and purified as described above.

Light chain phosphorylation and phosphorylation kinetics

To test whether the GFP fusion altered the phosphorylation of RLC by myosin light chain kinase (MLCK) we measured both the extent and the rate of phosphorylation of HMM bearing the GFP-RLC construct and compared these parameters to HMM that contains WT RLC. Electrophoresis on 40% glycerol-PAGE gels, which separates the phosphorylated RLC from the unphosphorylated species by charge, revealed that the GFP-RLC could be fully phosphorylated, but with slower kinetics than that obtained when using HMM with WT-RLC (Fig. 2a–b). These results were confirmed using a phosphorylation assay measuring the incorporation of ^{32}P into the light chain from [γ-^{32}P]ATP (Fig. 2c).

The phosphorylation kinetics were tested for the GFP-RLC-HMM IIA using [γ-^{32}P]ATP incorporation at different HMM concentrations where the initial rate of phosphorylation was measured (Fig. 3). There was no significant difference in the extrapolated maximal velocity, V_{max}, for myosin phosphorylation using MLCK (18.4 ± 1.9 s^{-1} for GFP-RLC-HMM vs. 20.6 ± 0.3 s^{-1} for WT-HMM, $P > 0.05$), however, there is a slight difference in the K_m (concentration of substrate required to give half maximal velocity) (2.1 ± 0.2 μM for WT-RLC vs. 3.6 ± 0.6 μM for GFP-RLC). Thus at low HMM concentrations the GFP-RLC-HMM will be phosphorylated more slowly than WT-HMM.

Steady state ATPase

To examine the enzymatic function of GFP-RLC-HMM IIA, steady-state MgATPase assays were performed as a function of actin concentration (Fig. 4). In the unphosphorylated state the GFP-RLC-HMM IIA has a basal ATPase activity with ~0.03 ± 0.01 s^{-1}, and after phosphorylation of the GFP-RLC by MLCK it increased in an actin dependent manner. The V_{max} was determined to be 0.20 ± 0.02 s^{-1} (mean ± SE, $n = 9$ individual series of experiments) which was significantly lower than we measured for WT-HMM IIA: 0.39 ± 0.02 s^{-1} (mean ± SE, $n = 8$; $P < 0.001$ with the pooled t-test) (Table 1, Fig. 4). There were no significant difference in the K_{ATPase}, which is the actin concentration at half maximal velocity and is an approximation of the actin affinity (9.53 ± 1.37 μM for GFP-RLC-HMM IIA compared to 7.97 ± 0.84 μM for WT-HMM IIA: $P > 0.1$ using the pooled t-test).

In vitro motility assays

The myosin motor function was tested for the ability to translocate fluorescently labeled actin filaments in an in vitro motility assay. Without MLCK treatment no movement of actin filaments were detected with either GFP-RLC-HMM IIA or WT-HMM IIA in the presence of ATP (data not show). Following phosphorylation, the actin filaments were moved at 0.29 ± 0.05 μm/s for the GFP-RLC-HMM IIA ($n = 155$ individual filaments were counted) versus 0.35 ± 0.06 μm/s for the WT-HMM IIA ($n = 79$) (Fig 5). The difference, albeit small, was significant by the two sample t-test ($P < 0.01$).

Discussion

The physiological functions and properties of the non-muscle myosin IIA were intensively investigated during the past decades using many different techniques in vitro and in vivo. One of the most useful in vivo methods involves cellular expression of the RLC fused to GFP. The GFP-RLC associates with the endogenous myosin and reports its location in living cells. In these experiments the GFP moiety could be fused to either the N- or the C-terminal regions of RLC. GFP fused to the C-terminal of the myosin regulatory light chain is widely used, and it was shown in vitro using smooth muscle myosin that this construct is regulated by phosphorylation and has normal enzymatic properties when fully phosphorylated (Komatsu et al. 2000). The kinetics of its phosphorylation by MLCK were not explored. Constructs in which GFP is fused to the N-terminus of RLC have also been

used in transient transfection studies and the light chain was incorporated into stress fibers presumably via its association with the myosin heavy chain (Peterson et al. 2004). However, the question of whether this fusion protein behaves similarly to endogenous RLC with respect to its effect on nonmuscle myosin's enzymatic and motile properties and its ability to regulate the enzymatic activity of the myosin has not been explored.

It was found that phosphorylation of the regulatory light chain of nonmuscle myosin IIA regulates not only the enzymatic activity of the molecule, but also the state of assembly (Scholey et al. 1980). In the absence of phosphorylation, nonmuscle myosin IIA forms filaments at physiological ionic strength in vitro when no ATP is present. Addition of ATP results in a depolymerization of the filaments and the soluble myosin adopts a conformation in which the tail folds back on the myosin heads to give a compact structure that sediments at 10S in the ultracentrifuge (Craig et al. 1983; Scholey et al. 1980; Umeki et al. 2009). Phosphorylation of the RLC stabilizes the filaments in the presence of ATP. More detailed analysis of the 10S myosin indicates that the two heads adopt an asymmetric conformation where the actin binding domain of one head binds to the base of the other head (Burgess et al. 2007; Jung et al. 2008; Umeki et al. 2009; Wendt et al. 1999, 2001). Electron paramagnetic spectroscopy and site directed spin labeling of the smooth muscle RLC suggest that the N-terminal phosphorylation domain of the RLC undergoes a conformational change upon phosphorylation, which increases the helical order, internal dynamics and accessibility (Espinoza-Fonseca et al. 2008; Nelson et al. 2005). This phosphorylation induced disorder-to-order transition is thought to lead to a decreased head-head interaction of the heavy chains, activating the motor domain.

The GFP molecule, which has a molecular weight approximately one and a half times that of the regulatory light chain itself, might possibly interfere with normal myosin function when fused to the amino-terminus of RLC. It might block the ability of MLCK to phosphorylate ser-19, prevent the myosin from adopting the off state conformation, or interfere with normal enzymatic or mechanical function of the myosin. We found that the myosin containing the GFP-RLC has a very low MgAT-Pase activity in the presence of actin when it is in the unphosphorylated state. This rate is very similar to that of WT-HMM IIA suggesting that the molecule is able to adopt the folded off state. The GFP-RLC-HMM IIA was also incapable of moving actin filaments in the unphosphorylated state. The GFP-RLC bound to HMM IIA was phosphorylated by MLCK with virtually the same V_{max}, albeit with a higher K_m as was obtained using WT-HMM IIA. This means that at low myosin concentrations, the GFP-RLC would be phosphorylated more slowly than the WT-RLC, however, at high myosin concentrations this difference would not be apparent.

The MgATPase activity of GFP-RLC-HMM IIA was markedly activated by phosphorylation, again suggesting that the chimeric molecule is well regulated by phosphorylation. However, the V_{max} of the actin-activated MgAT-Pase activity for phosphorylated GFP-RLC HMM IIA was only about half of the WT-HMM IIA. The $K_{ATPase,}$ which is an approximation of the affinity of the HMM for actin, was not greatly affected by choice of RLC. The rate of actin filament sliding generated by phosphorylated GFP-RLC-HMM IIA was also somewhat slower than that of WT-HMM IIA. The observation that the actin-activated MgATPase activity is more compromised by the GFP fusion, than the rate of actin filament sliding is explained by the fact that these two measurements are likely controlled by two different kinetic steps. The actin-activated MgATPase rate of HMM IIA is limited by phosphate release (Kovacs et al. 2003), whereas the rate of actin filament sliding is thought to be limited by ADP release (Siemankowski et al. 1985).

The differences we found in the kinetics and phosphorylation dynamics of the GFP fused RLC are not large and should not preclude the use of this fluorescent-fusion protein in cell biological studies. Mutation studies have demonstrated that some myosin mutations that alter function in vitro are able to support their in vivo functions to various degrees. A mouse where the endogenous myosin IIB has been replaced by a mutation that has only 25% of its normal actin-activated MgATPase in vitro is viable, albeit with some phenotypic manifestations (Kim et al. 2005; Ma et al. 2004). Similarly, many in vitro function altering mutations in the *Dictyostelium* myosin II support functions in the living organism, sometimes with little obvious phenotypes (Ruppel and Spudich, 1996). The fact that the enzymatic activity of the GFP-RLC-HMM IIA used in this study is still regulated by phosphorylation implies that full length nonmuscle myosin should be able to adopt the off state and probably form the 10S conformation that may be necessary for dynamic myosin localization in cells. Thus, the N-terminal GFP-tagged RLC does not drastically affect the in vitro properties of nonmuscle myosin and that its use as a fluorescent-fusion protein for imaging the localization of myosin in cells is justified.

Acknowledgments

RLC acknowledges the support of NIH grant GM39264.

HMM IIA baculovirus was made by Mihály Kovács. We thank Mary Anne Conti and Mitsuo Ikebe for the gift of MLCK used in these experiments, Fang Zhang for excellent technical assistance and Attila Nagy for comments on the manuscript.

References

Bajaj G, Zhang Y, Schimerlik MI, Hau AM, Yang J, Filtz TM, Kioussi C, Ishmael JE. N-methyl-D-aspartate receptor subunits are non-myosin targets of myosin regulatory light chain 1. J Biol Chem. 2009; 284:1252–1266. [PubMed: 18945678]

Bresnick AR. Molecular mechanisms of nonmuscle myosin-II regulation. Curr Opin Cell Biol. 1999; 11:26–33. [PubMed: 10047526]

Burgess SA, Yu S, Walker ML, Hawkins RJ, Chalovich JM, Knight PJ. Structures of smooth muscle Myosin and heavy meromyosin in the folded, shutdown state. J Mol Biol. 2007; 372:1165–1178. [PubMed: 17707861]

Craig R, Smith R, Kendrick-Jones J. Light-chain phosphorylation controls the conformation of vertebrate non-muscle and smooth muscle myosin molecules. Nature. 1983; 302:436–439. [PubMed: 6687627]

Espinoza-Fonseca LM, Kast D, Thomas DD. Thermodynamic and structural basis of phosphorylation-induced disorder-to-order transition in the regulatory light chain of smooth muscle myosin. J Am Chem Soc. 2008; 130:12208–12209. [PubMed: 18715003]

Facemyer KC, Cremo CR. A new method to specifically label thiophosphorylatable proteins with extrinsic probes. Labeling of serine-19 of the regulatory light chain of smooth muscle myosin. Bioconjug Chem. 1992; 3:408–413. [PubMed: 1420439]

Homsher E, Wang F, Sellers JR. Factors affecting movement of F-actin filaments propelled by skeletal muscle heavy meromyosin. Am J Physiol Cell Physiol. 1992; 262:C714–C723.

Jung HS, Burgess SA, Billington N, Colegrave M, Patel H, Chalovich JM, Chantler PD, Knight PJ. Conservation of the regulated structure of folded myosin 2 in species separated by at least 600 million years of independent evolution. Proc Natl Acad Sci USA. 2008; 105:6022–6026. [PubMed: 18413616]

Kim KY, Kovacs M, Kawamoto S, Sellers JR, Adelstein RS. Disease-associated mutations and alternative splicing alter the enzymatic and motile activity of nonmuscle myosins II-B and II-C. J Biol Chem. 2005; 280:22769–22775. [PubMed: 15845534]

Komatsu S, Yano T, Shibata M, Tuft RA, Ikebe M. Effects of the regulatory light chain phosphorylation of myosin II on mitosis and cytokinesis of mammalian cells. J Biol Chem. 2000; 275:34512–34520. [PubMed: 10944522]

Kovacs M, Wang F, Hu A, Zhang Y, Sellers JR. Functional divergence of human cytoplasmic myosin II: kinetic characterization of the non-muscle IIA isoform. J Biol Chem. 2003; 278:38132–38140. [PubMed: 12847096]

Ma X, Kawamoto S, Hara Y, Adelstein RS. A point mutation in the motor domain of nonmuscle myosin II-B impairs migration of distinct groups of neurons. Mol Biol Cell. 2004; 15:2568–2579. [PubMed: 15034141]

Nelson WD, Blakely SE, Nesmelov YE, Thomas DD. Site-directed spin labeling reveals a conformational switch in the phosphorylation domain of smooth muscle myosin. Proc Natl Acad Sci USA. 2005; 102:4000–4005. [PubMed: 15753305]

Nishikawa M, Sellers JR, Adelstein RS, Hidaka H. Protein kinase C modulates in vitro phosphorylation of the smooth muscle heavy meromyosin by myosin light chain kinase. J Biol Chem. 1984; 259:8808–8814. [PubMed: 6235218]

Peterson LJ, Rajfur Z, Maddox AS, Freel CD, Chen Y, Edlund M, Otey C, Burridge K. Simultaneous stretching and contraction of stress fibers in vivo. Mol Biol Cell. 2004; 15:3497–3508. [PubMed: 15133124]

Rayment I, Rypniewski WR, Schmidt-Bäse K, Smith R, Tomchick DR, Benning MM, Winkelmann DA, Wesenberg G, Holden HM. Three-dimensional structure of myosin subfragment-1: A molecular motor. Science. 1993; 261:50–58. [PubMed: 8316857]

Ruppel KM, Spudich JA. Structure-function studies of the myosin motor domain: importance of the 50-kDa cleft. Mol Biol Cell. 1996; 7:1123–1136. [PubMed: 8862525]

Scholey JM, Taylor KA, Kendrick-Jones J. Regulation of non-muscle myosin assembly by calmodulin-dependent light chain kinase. Nature. 1980; 287:233–235. [PubMed: 6893621]

Sellers JR. Regulation of cytoplasmic and smooth muscle myosin. Curr Opin Cell Biol. 1991; 3:98–104. [PubMed: 1854490]

Sellers JR. Myosins: a diverse superfamily. Biochim Biophys Acta. 2000; 1496:3–22. [PubMed: 10722873]

Sellers JR. In vitro motility assay to study translocation of actin by myosin. Curr Protoc Cell Biol. 2001; Chapter 13(Unit 13.2)

Sellers JR, Soboeiro MS, Faust K, Bengur AR, Harvey EV. Preparation and Characterization of Heavy Meromyosin and Subfragment 1 from vertebrate cytoplasmic myosins. Biochemistry. 1988; 27:6977–6982. [PubMed: 2973809]

Siemankowski RF, Wiseman MO, White HD. ADP dissociation from actomyosin subfragment 1 is sufficiently slow to limit the unloaded shortening velocity in vertebrate muscle. Proc Natl Acad Sci USA. 1985; 82:658–662. [PubMed: 3871943]

Uchimura T, Fumoto K, Yamamoto Y, Ueda K, Hosoya H. Spatial localization of mono-and diphosphorylated myosin II regulatory light chain at the leading edge of motile HeLa cells. Cell Struct Funct. 2002; 27:479–486. [PubMed: 12576640]

Umeki N, Jung HS, Watanabe S, Sakai T, Li XD, Ikebe R, Craig R, Ikebe M. The tail binds to the head-neck domain, inhibiting ATPase activity of myosin VIIA. Proc Natl Acad Sci USA. 2009; 106:8483–8488. [PubMed: 19423668]

Vicente-Manzanares M, Ma X, Adelstein RS, Horwitz AR. Non-muscle myosin II takes centre stage in cell adhesion and migration. Nat Rev Mol Cell Biol. 2009; 10:778–790. [PubMed: 19851336]

Wang F, Harvey EV, Conti MA, Wei D, Sellers JR. A conserved negatively charged amino acid modulates function in human nonmuscle myosin IIA. Biochemistry. 2000; 39:5555–5560. [PubMed: 10820029]

Wang F, Kovacs M, Hu AH, Limouze J, Harvey EV, Sellers JR. Kinetic mechanism of non-muscle myosin IIB—functional adaptations for tension generation and maintenance. J Biol Chem. 2003; 278:27439–27448. [PubMed: 12704189]

Wendt T, Taylor D, Messier T, Trybus KM, Taylor KA. Visualization of head-head interactions in the inhibited state of smooth muscle myosin. J Cell Biol. 1999; 147:1385–1390. [PubMed: 10613897]

Wendt T, Taylor D, Trybus KM, Taylor K. Three-dimensional image reconstruction of dephosphorylated smooth muscle heavy meromyosin reveals asymmetry in the interaction between myosin heads and placement of subfragment 2. Proc Natl Acad Sci USA. 2001; 98:4361–4366. [PubMed: 11287639]

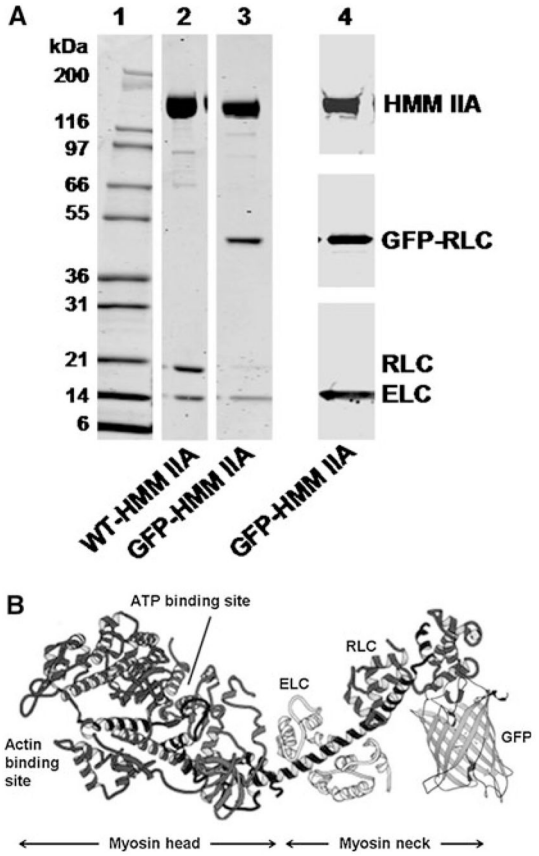

Fig. 1.

Purified proteins used in the study. **a** Coomassie Blue stained SDS–polyacrylamide gels of *Lane* 1 Molecular weight standards; *Lane* 2 WT-HMM IIA; *Lane* 3 GFP-RLC-HMM IIA. *Lane* 4 shows the composite results of western blots of GFP-RCL-HMM IIA for anti-Flag antibody which recognizes the Flag-tagged HMM IIA heavy chain, anti-GFP which recognizes the GFP-RLC and anti-ELC antibodies which recognizes the ELC. **b** Hypothetical structure of the single HMM head with the GFP-RLC. Modified after the original image by Rayment et al. (1993). Please note that this is taken from the crystal structure of chicken skeletal muscle subfragment one where the N-terminal 18 amino acids of the RLC were not visualized. Thus, the exact localization of the GFP fusion protein cannot be determined. The figure is meant instead to show the relative size of GFP compared to the RLC

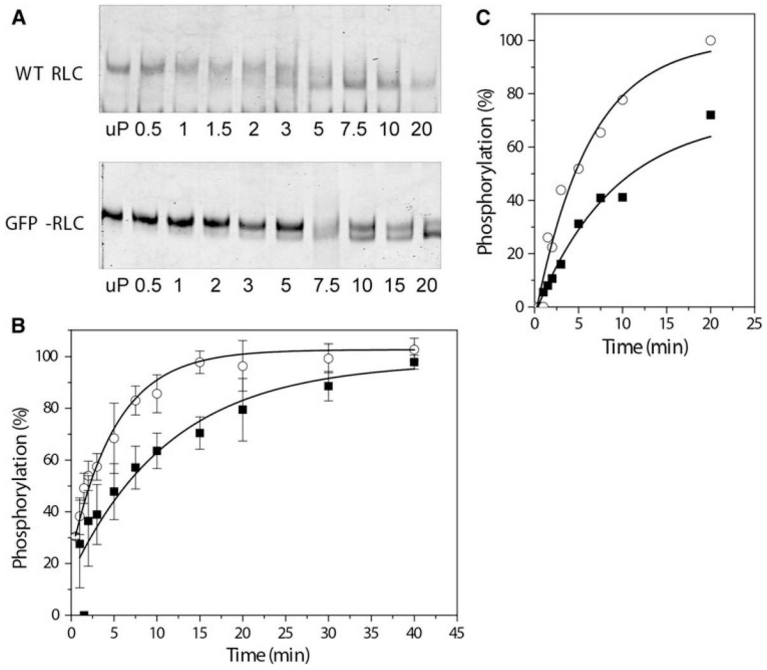

Fig. 2.

Time course of phosphorylation of WT-RLC or GFP-RLC bound to HMM IIA. Conditions are described in Materials and Methods section. The reaction was initiated by addition of 0.0136 μg/ml MLCK, **a** 40%-Glycerol-polyacrylamide gels of the WT-RLC (*upper gel*) or GFP-RLC (*lower gel*) showing the shift to higher mobility that accompanies phosphorylation. The scale is in minutes. Unphosphorylated (up) HMM (with either WT-RLC or GFP-RLC) is in the far left *Lane* of both gels. **b** Determination of the extent of phosphorylation by densitometry scanning of gels such as those shown in panel A for WT-HMM IIA (*circles*) or GFP-RLC-HMM IIA (*squares*). **c** RLC phosphorylation measured with [γ-^{32}P]ATP. WT-HMM IIA (*circles*) or GFP-RLC-HMM IIA (*squares*). Values are presented with ± SE, $n = 4$ series of data

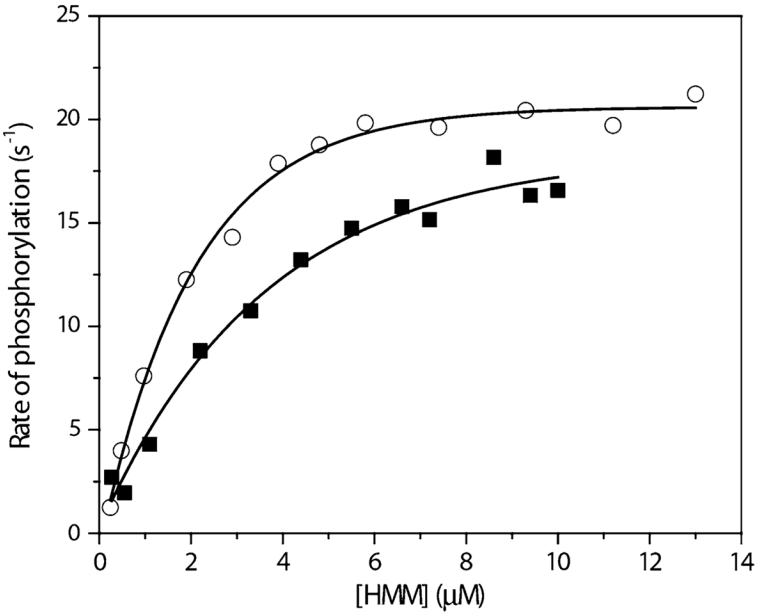

Fig. 3.

Rate of phosphorylation of WT-HMM IIA and GFP-RLC-HMM IIA. The initial rate of phosphorylation of the proteins were measured as described in Materials and Methods after addition of various concentrations of WT-HMM IIA (*circles*) or GFP-RLC-HMM IIA (*squares*) at 0.0136 μg/ml MLCK, using [γ-^{32}P]ATP. Data were fit to the Michaelis–Menten equation to determine V_{max} and K_m. The Chi-square test was used for statistical analysis and shows no significant difference in the V_{max} of phosphorylation for GFP-RLC-HMM IIA versus WT-HMM IIA ($P > 0.05$)

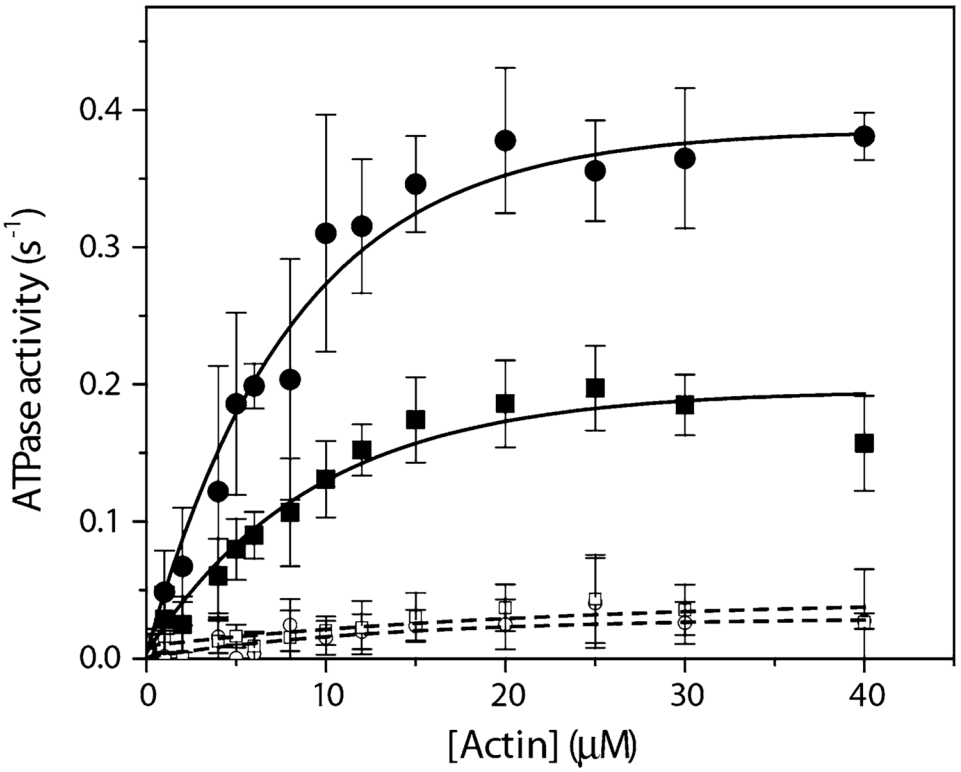

Fig. 4.

Steady state actin-activated MgATPase activity of WT-HMM IIA and GFP-RLC-HMM IIA. The MgATPase activity of either phosphorylated or unphosphorylated HMM IIA was measured by a NADH-coupled assay at various actin concentrations as described in Materials and Methods. *Closed circles* represent phosphorylated WT-HMM IIA; *closed squares* represent phosphorylated GFP-RLC-HMM IIA; *open circles* represent unphosphorylated WT-HMM IIA; *closed squares* represent unphosphorylated GFP-RLC-HMM IIA. The results are the summary of at least eight individual protein preparations. All data are presented with ± SE, $n = 8$

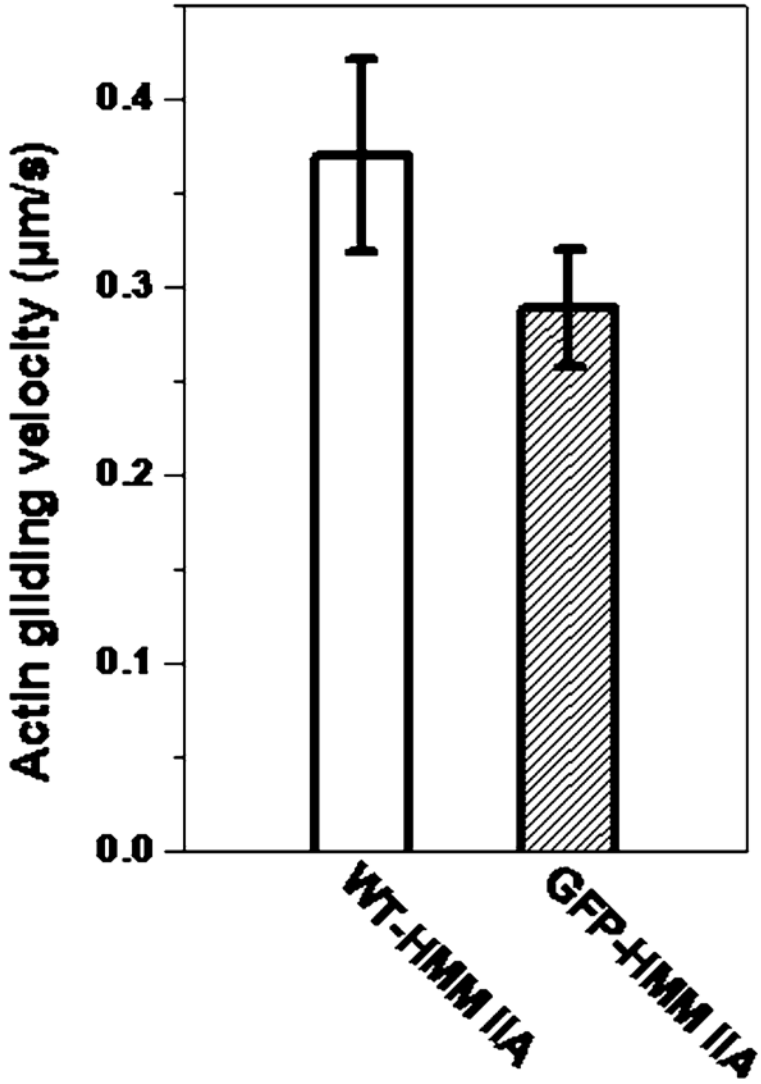

Fig. 5.

In vitro gliding assay of phosphorylated WT-HMM IIA and GFP-RCL-HMM IIA. Conditions are as described in Materials and Methods. Bars show the velocity of actin filament gliding over surfaces coated with either WT-HMM IIA or GFP-RLC-HMM IIA after phosphorylation with MLCK. No movement was observed in the absence of phosphorylation. The values shown are mean velocity ± SE, of at least 65 individual filaments were measured for each molecule

Table 1

Kinetic data of the steady-state ATPase assay of WT and GFP-HMM IIA after exponential fit

	Unphosphorylated		Phosphorylated (3.6 μg/ml MLCK)		
	−Actin	+Actin	−Actin	+Actin	
	V_{max} (s^{-1})	V_{max} (s^{-1})	V_{max} (s^{-1})	V_{max} (s^{-1})	K_{ATPase} (μM)
WT-HMM IIA	0.006 ± 0.01	0.026 ± 0.01	0.006 ± 0.01	0.39 ± 0.016	7.97 ± 0.84
GFP-HMM IIA	0.004 ± 0.002	0.029 ± 0.007	0.003 ± 0.005	0.20 ± 0.02	9.53 ± 1.37

All data are presented with ± SE

J Muscle Res Cell Motil. Author manuscript; available in PMC 2013 September 30.